On the potential wet self-cleaning and spectral transmittance of snakes' spectacle

Weibin Wu[1,2,*], KM Samaun Reza[1,*], Dmitry Busko[1], Felix Buck[1], Richard Thelen[1], Guillaume Gomard[3], Hendrik Hölscher[1,+]

[1] *Institute of Microstructure Technology (IMT), Karlsruhe Institute of Technology (KIT), Hermann-von-Helmholtz-Platz 1, 76344 Eggenstein-Leopoldshafen, Germany*

[2] *Institute of Noise and Vibration, Naval University of Engineering, Wuhan 430033, P. R. China*

[3] *Carl Zeiss AG, ZEISS Innovation Hub @ KIT, Hermann-von-Helmholtz-Platz 6, 76344 Eggenstein-Leopoldshafen, Germany*

[*] *Both authors contributed equally to this work*

[+] *hendrik.hoelscher@kit.edu*

Date: 8th of August 2026

Abstract: The eyes of snakes are protected by transparent scales, commonly called "spectacles" or "brille". As is widely known, snakes have no eyelids or other extremities to clean their eyes. Therefore, we test the hypothesis that their spectacle scales feature surface structures for self-cleaning. Additionally, snakes' spectacle scales might be optimized through evolution to enhance light capturing by the retina. To address these two subjects, we characterize the spectacle scales of 18 snake species belonging to 5 families regarding their wettability, adhesion, spectral transmittance, and micro-ornamentation utilizing optical spectroscopy, contact angle measurements, scanning electron microscopy, and atomic force microscopy. Remarkably, the optical transmittance of spectacle scales is moderate, with values of 70% to 90% above 400 nm. In most cases, the transmittance of spectacle scales is not significantly better than transparent dorsal or ventral scales. Furthermore, the spectacle scales are only slightly hydrophobic, with contact angles between 90° and 105°. In general, the contact angles are even lower than on dorsal and ventral scales. These results can be explained by the fact that the surface geometries of spectacle' scales are flat down to the nanoscale, comprising only polygonal cracks and nanoscale pits. Therefore, we conclude that snakes' spectacle scales do not feature advantageous properties regarding wet self-cleaning and optical transmittance. Additionally, we explain the physical origin of a transmittance peak close to 254 nm observed for scales of various snake species by the fluorescence of keratin.

Keywords: snakes, scales, spectacle scales, optical transmittance, fluorescence keratin

Introduction

The eyes of snakes, fossorial lizards, and most geckos are covered by a transparent scale, the so-called spectacle scale (Lillywhite, 2014; van Doorn and Sivak, 2015; Collin et al., 2025). It is released as part of the snakes' shed skin together with all other scales (see Figure 1) and mechanical protection of the cornea, minimization of evaporative water loss, and protection against solar radiation are its primary functions (Lillywhite, 2014; Walls, 1934). The spherical shaped spectacle scales are the hard integument of several layers of α- and β-keratin, respectively (van Doorn et al., 2014). As an example, Figure 1 shows photographs of head scales moulted from *V. aspis* and *B. arietans*. In both photographs, the spectacles appear significantly more transparent than the other head scales, indicating high spectral transmittance. Furthermore, they are slightly larger than the other scales and feature a round outer shape.

Most studies on snake eyes published so far focused on their morphology or anatomy (Cazalot et al., 2015; Da Silva et al., 2016; Da Silva et al., 2017; Guerra-Fuentes et al., 2014; Lauridsen et al., 2014). Nonetheless, the functionality of spectacles of snakes and lizards was already discussed in 1934 by Walls (1934) but only a few studies followed. In 1999, Campbell et al. (1999) conducted an extensive study on the pit organ, spectacles, and other scales of the carpet python *(Morelia spilota)* utilizing atomic force microscopy (AFM) and scanning electron microscopy (SEM). They observed tiny dimples – commonly named micropits - of different diameters (some 100 nm) and depths (some 10 nm) on all scales. Interestingly, these micropits are largest on the pit organ scale, and the authors concluded that the size distribution of these structures on the pit organ might enhance light scatter in the visible regime. However, enhanced optical features of the spectacles were not reported.

In the last decade, a few studies measured the spectral transmittance of spectacles in the visible and ultraviolet (UV) spectrum on several snake species (Hart et al., 2012; Simoes et al., 2016; van Doorn, 2012; van Doorn and Sivak, 2015). A high-pass for visible light but a cut-off in the UV regime was observed for the spectacles of the two sea snakes *Lapemis curtus* and *Acalyptophis peronii* (Hart et al., 2012), 43 terrestrial snake species (van Doorn and Sivak, 2015) as well as 11 primarily diurnal, and 8 not primarily diurnal snakes (Simoes et al., 2016). This UV filter function is believed to serve as protection against solar radiation, but a taxonomic variation of the cut-off wavelength was observed. Van Doorn et al. (2014) analysed the keratin composition of the spectacles of snakes and geckos. They concluded that there is no direct

correlation between keratin content and transparency. Nonetheless, they observed that the composition of spectacles is different compared to other scales. Furthermore, they reported an absence of beta-keratin in the spectacles of geckos, what might cause a wider transparency range compared to snakes (van Doorn and Sivak, 2015).

Another interesting question is if and how snakes clean their spectacles. Although they locomote in direct contact with the ground with unavoidable dust or other contaminations all around, they do not have any extremities for wiping their eyes. Some lizards are known to clean their eyes with their tongues, but we could not find any evidence that snakes have this ability. Therefore, we investigated the wettability of the spectacles to learn about possible self-cleaning properties. A previous study by Autumn & Hansen (2006) on the *Gekko gecko* showed that the equilibrium water contact angle on living geckos and isolated spectacles are (98.3 $\pm$ 3.4)° and (93.3 $\pm$ 3.5)°, respectively. Such values are commonly considered too low to guarantee self-cleaning properties via the so-called lotus effect (Barthlott et al., 2016). Consequently, it is of high interest to check whether the wetting properties of the snakes' spectacles are sufficient for wet self-cleaning.

As an illustrative demonstration, Figure 2 shows photos of water droplets on the spectacle scales of a living *Python regius*. The contact angle is roughly about 100° (see inset in Fig. 2C), but the water droplets do not roll-off as it would be expected for wet self-cleaning. Figure 2B) shows an event where two droplets stick to both spectacles. Most likely, such observations were occasionally made by many snake keepers moisturizing the skin of their snakes by spraying them with water for various reasons, but such anecdotical incidents did not make it into scientific literature so far.

To address the two research questions discussed above, we characterized the wetting and optical properties of the spectacles of 18 snake species from five families (see Table 1). In general, all scales are only slightly hydrophobic, with contact angles of around 100°. Such values are not high enough to enable wet self-cleaning properties as found on other natural surfaces like lotus leaves with self-cleaning effects. Furthermore, we measured the optical transmission of the spectacles in the visible and ultraviolet regimes. They feature only moderate transmittance of about 70% to 90% in the visible regime and a cut-off in the UV regime. A peak in the lower UV spectrum around 254 nm (van Doorn, 2012) is shown to be caused by a fluorescence effect of keratin. To confirm that there are no dedicated structures on the exterior surface of the spectacles, we characterized them by scanning electron microscopy (SEM) and atomic force microscopy (AFM). In general, we observed a flat surface topology containing

only nanoscale topography features like polygonal cracks and micropits. This flatness is in accordance with the observed low contact angles and moderate transmission values.

Methods

Sample preparation

Topological, wetting, adhesion, and optical properties of the moulted spectacles of eighteen snake species across five different families with various diurnal/nocturnal activities are presented in this study. The moulted skins (mostly N = 1, i.e., 2 spectacle scales per species) from captive snakes were collected by G. Gomard thanks to the contribution of different snake keepers listed in the Acknowledgements. The moulted scales belonged to snakes from different geographical locations and habitats. Their respective family, geographical origin, and habitat are summarized in Table 1. For contact angle measurements and SEM imaging, the scales were secured on a silicon and glass substrate with conductive adhesive tape (Plano GmbH, Wetzlar, Germany). For the AFM imaging, the scales were sequentially cut into small pieces and fixed on a glass substrate with two-component glue (UHU Plus Endfest 300). After preparation, the samples were carefully cleaned with pressurized air. Temperature (21°C – 23°C) and humidity (50% - 70%) were well controlled during storage and measurements of all samples.

Characterization techniques

The water contact angle (CA) measurement was conducted with an OCA 40 system, and the CA was calculated utilizing the corresponding SCA20 software (DataPhysics Instruments, Germany) with the Young-Laplace fitting method. The droplet volume was 1 µL, and the dispensing speed was 0.5 µL/s. The resulting contact angles were averaged from 12 measurements, and the corresponding standard deviation was calculated from these.

The total spectral transmittance was recorded with a LAMBDA 1050 UV-vis spectrophotometer with an integrating sphere attachment for diffused transmittance and reflectance measurement (PerkinElmer Inc., USA). The optical spectrum was measured from 200 nm or 300 nm up to 800 nm with a spectral resolution of 1 nm, 2 nm, or 5 nm, respectively, and a beam spot diameter of 1 mm. The spectrophotometer was calibrated by defining the transmittance in air without placing any sample between the detector and the light source as 100% transmittance. For comparison, we extracted the total spectral transmission at the upper limit of the visible at 750 nm as $T_{@750\text{nm}}$. Afterwards, this value served as the reference value to determine the wavelength $\lambda_{50\%}$ where the transmission reduced to 50% in the UV. All values are summarized in Table 1.

The fluorescence emission of the snake scales was measured using an irradiance calibrated CCD spectrometer (AvaSpec-ULS2048x64TEC-EVO, Avantes BV) under an excitation by 268 nm LED (UV-LED iSFL, Opsytech). The emission was collected by a bare optical fibre with a diameter of 1 mm (Orion). The different size of specimens and their fragility did not allow a quantitative comparison of an emission strength from different scales.

The scale ornamentations were imaged by scanning electron microscopy (SUPRA 60 VP, Zeiss, Germany) after sputtering a thin silver layer. The imaging was conducted with an acceleration voltage of 3 kV, and the detector was placed at a working distance between 5 mm and 7 mm.

The topography of spectacles was further analysed by atomic force microscopy (Dimension Icon AFM, Veeco Inc., USA) with rectangular cantilevers (All-in-One-Al, BudgetSensors). Spring constant and deflection sensitivity of the cantilevers were determined with the thermal tune method integrated into the commercial AFM software. The adhesion forces between the tip and scales were measured with a ramp rate of 1 µm/s.

Results

Wetting properties of snake scales

Numerous studies have been conducted to investigate the wet self-cleaning properties described for lotus leaves and many other natural surfaces (Barthlott et al., 2016). In most cases, hierarchical combinations of micro- and nanostructures reduce the effective surface energy for water droplets, resulting in high contact (> 150°) and low roll-off angles (< 10°). When water droplets fall onto lotus leaves, they form spherical drops and roll off the surfaces, collecting debris and other particles. Inspired by this famous self-cleaning effect, we studied the wetting properties of spectacles to address the question of if and how snakes clean their eyes. For completeness, we also examined the contact angles on dorsal and ventral scales of the respective snake species (Buck, 2020).

As a representative example, Figure 3 shows photos of a 1 µL water droplet on the dorsal, ventral, and spectacle scales of *S. m. barbouri* revealing the angles of 143°, 111°, and 103°, respectively. The contact angle on the dorsal scale is highest. Surprisingly, it is the smallest on the spectacles, where one might expect a high value for wet self-cleaning. The contact angle on the ventral scale lies in between. All determined contact angles are summarized in Table 1.

For several snakes, we observe the same trend for the contact angles of their scales. The dorsal ones feature the largest contact angles, while they are lowest on the spectacles, and intermediate values are found on the ventral scales. This ranking is most likely caused by the height of the respective micro-ornamentations. Regarding the dorsal scales, the most hydrophobic species are *B. arietans*, *S. m. barbouri* and *V. aspis* with an average contact angle of over 140°, while *M. monspessulanus*, *V. u. rakosiensis*, *P. schultzei*, *N. atra*, *T. honsonensis* and *S. diadema* exhibit contact angles between 120° and 130°. Intermediate values between 130° and 140° are observed on the dorsal scales of *M. spilota* and *P. guttatus*. Most snakes exhibit a contact angle of nearly 110° on their ventral scales, except for *M. monspessulanus* (118°). On spectacles, however, the contact angles are typically close to 100°. The smallest value of 86° is observed on the aquatic snake *N. tessellata*.

Interestingly, there are some snake scales in our compilation that show complete wetting, *i.e.*, water droplets spread and wet the surface completely when dropped on some scales. The dorsal scales of *T. subannulatus*, for example, get completely wet, and the ventral scales are hydrophilic with a contact angle of 60°.

It is somehow unexpected that snake spectacle scales do not feature a high contact angle for water, which would potentially allow wet self-cleaning. For a flat surface, a low water contact angle corresponds to high adhesion energy (or force) of the surface (Butt and Kappl, 2010). Therefore, to further verify this finding, we additionally measured the forces acting on a probing tip while it is pulled away from the scales' surfaces. This adhesion force correlates with the wetting behaviour and is mostly caused by van-der-Waals forces. We measured these on the dorsal, ventral, and spectacle scales of 9 snakes with an atomic force microscopy (AFM) with a sharp silicon tip (Wu, 2020). The results obtained on this subset of the 18 examined species are compared in Figure 4.

For all investigated snakes, the largest adhesion force was observed on the spectacle scales. It is smallest on the dorsal scales, while adhesion on ventral scales is in-between. This outcome agrees with the typical surface geometries. The adhesion is largest on the practically flat spectacles and smallest on the dorsal scale which typically feature surface structure with increased height, while the ventral scales are in-between. Consequently, the overall distribution of adhesion values confirms the low water contact angles on spectacles reported above.

As a low contact angle results in a high roll-off angle, we conclude that most snakes do not feature potential wet self-cleaning of their spectacles through the lotus effect. Nonetheless, with contact angles at least close to super-hydrophobicity, the dorsal scales of snakes are still

potential candidates for a wet self-cleaning effect. The spectacle scales, however, cannot provide this ability.

Spectral transmittance of spectacles

Since spectacles feature no properties for wet self-cleaning, it might be assumed that self-cleaning is sacrificed to achieve enhanced spectral visibility. We, therefore, examined the optical transmittance of the spectacle scales. Figure 5 summarizes the resulting spectra for all eighteen species. In Figure 5A) and B), the transmittance is shown for the range of 200 nm to 800 nm, while the spectra in C) were recorded in a reduced range of 300 nm to 800 nm. The overall features of the spectra agree with previous studies (Hart et al., 2012; Simoes et al., 2016; van Doorn, 2012; van Doorn and Sivak, 2015).

In general, the transmittance of the spectacles has constant values around 70% to 90% for wavelength larger than 400 nm. This range widely coincides with the visible range of humans (380 nm to 750 nm), but the visibility range of snakes might be different, depending on the respective species (Simoes et al., 2016). However, the transmittance starts to decrease in the UV-A regime (315 nm to 400 nm) and reduces to 50% for wavelengths between 300 nm and 330 nm. An exception is *N. atra*; for this snake, the value of $\lambda_{50\%}$ is 385 nm (see Table 1). Here, it is interesting to note that higher $\lambda_{50\%}$-values were also reported for *Naja annulifera* and *Naja pallida* by van Doorn and Sivak (2015). So, this higher cut-off might be typical of cobras or members of the family Elapidae. Additionally, we also observe that the cut-offs of Colubridae are mostly slightly higher than for Viperidae. Nonetheless, the entirety of all spectra confirms that all spectacles feature a wide transparency range, ensuring clear vision for most snakes partly even in the UV-A regime. However, as pointed out by other authors already, the transmittance in the UV-B regime (280 nm to 315 nm) decays steeply (Hart et al., 2012; Simoes et al., 2016; van Doorn, 2012; van Doorn and Sivak, 2015) and reduces close to zero for wavelengths in the UV-C regime (below 280 nm). This high absorption suggests that the spectacles work as a UV-B and -C filter, protecting the inner tissue of the eye from harmful radiation.

Additionally, it is interesting to note that for various species, the transparency of the spectacles is not superior to ventral scales. Some snakes have ventral scales which appear transparent or translucent to the naked eye, too (Reza et al., 2025). Figure 6 compares the total transmittance spectra of dorsal, ventral, and spectacle scales of eight species. In six cases, the transmittance values and the overall shape of the spectra of ventral scales are very close to the respective spectacle scales. Dorsal scales, which typically contain melanin, are less transparent

in the visible range. Nonetheless, the agreement of the ventral and spectral spectra suggests that the keratin of the spectacles is not superior to ventral scales regarding optical properties.

Finally, it is interesting to emphasize the UV transmission peak around 254 nm in various transmittance spectra. The effect is most prominent for the spectacles of *P. schultzei* and *T. honsonensis* (see Figure 5B). We observed this peak as well for dorsal and ventral scales of several snake species (Reza, 2025) and it has been reported by other authors (van Doorn, 2012; van Doorn and Sivak, 2015). After validating that this peak is not an artifact of the utilized spectrometer(s), we considered several possible reasons for that observation; finally confirming that the peak is caused by the fluorescence of keratin excited by a UV-C probe light. The fluorescence spectra of scales were separately measured under a UV light excitation (268 nm LED) (see Figures 5D and 7). The most pronounced fluorescence, ranging from 300 up to 800 nm, was detected from *P. schultzei* dorsal scales, that have also shown the most intense transmission peak, as noted above. The origin of this "transmission" peak caused by a fluorescence can be described as following. The detector of the spectrophotometer cannot distinguish between the probing light and a broadband fluorescence emitted by a sample and, therefore, a total light amount in the integrating sphere is treated as a whole. The light added by fluorescence is measured as an apparent increase in transmission signal (or equivalently, a decrease in absorption). If the transmission is measured at 250 nm, for example, the probing light source shines light of 250 nm on the spectacle scale but the detector in a common spectrometer additionally collects all excited wavelengths caused by the fluorescence (not only the 250 nm signal). In some cases, due to differences in a detector sensitivity to UV light and to the fluorescence emission, the transmission values given by a spectrophotometer could potentially exceed 100%, that would be a most clear indication of an artifact presence. It is important to note that this effect is different to bio-fluorescence observed in various reptiles and amphibians (Prötzel et al., 2018; Lamb and Davis, 2020; Paul and Mendyk, 2021; Prötzel et al., 2021; Alvarez et al., 2022; Botelho et al., 2024).

Micro-ornamentations on the spectacles

All studied spectacles looked perfectly smooth to the naked eye. Nonetheless, characterizing their surfaces by scanning electron microscopy and atomic force microscopy, we still observe some nanoscale features. As an example, Figure 8 displays SEM images of a spectacle of *P. guttatus*. Figures 8A) and B) compare the topography in the central region with the margin of the spectacle, respectively. Stitching micro-ornamentations of pentagons or hexagons with a diameter of 20-30 μm are found in both regions. Nonetheless, as reported by Collin et al. (2025)

the overall structure of the periphery and the centre region differ. For completeness, we also imaged a cross-section of the scale (Fig. 8C). In that cut, we only observed thin layers without any obvious structure.

To obtain a detailed height analysis of the topology, we also recorded AFM images on several spectacles (see Figure 9). For *P. guttatus*, we observe now two different polygon borders forming channels (darker colours) and elevated stitching boundaries (lighter colours) in Figure 9A). The narrow channels resemble very shallow dents with a depth of around 15 nm. However, the stitching boundaries are ridges with a height of around 20 nm. Interestingly, in the enlarged image Figure 9B) microfibril structures are observed at the stitching boundaries. These resemble the fibrillar structure found on the ventral scales of many snakes but their height is greatly lower (Wu et al., 2020). However, such structures are absent on the channel borders. In addition to narrow channels and stitching boundaries, numerous nanoscale depressions are observed. These tiny dimples are about 100 nm in diameter and 10 nm in depth, *i.e*., their overall size agrees roughly with the sizes reported for the carpet python (Campbell et al., 1999).

A quite similar surface morphology is observed on the spectacles of *V. u. rakosiensis* and *N. atra* as shown in Fig. 9C) and D). Stitching boundaries and narrow channels are also observed on the spectacles of *V. u. rakosiensis.* However, the dimensions of the observed surface structures vary among species. Narrow channels and stitching boundaries with depth and height around 30 nm are found on the spectacles of *V. u. rakosiensis*. Nanoscale pits observed on the spectacles, have a diameter between 120 nm and 160 nm as well as a depth between 10 nm and 15 nm. As shown in Figure 9D), numerous micropits are also found on the spectacles of *N. atra*. However, these are deeper than on the previously presented scales. Here, the diameter and depth of the micropits are about 150 nm and 30 nm, respectively.

The surface topography of the spectacles of *T. honsonensis* is presented in Figure 9E) and F). Narrow channels and stitching boundaries are not prominent on the scales of this species, but a high density of micropits can be observed (Fig. 9F). The density of these is higher compared to the ones found on the scales of *P. guttatus, V. u. rakosiensis* and *N. atra*. Their diameter and depth are around 300 nm and 30 nm, respectively. These values are larger and deeper as observed on the previously discussed spectacles. A similar surface topology is also detected on the scales of *P. schultzei* (Fig. 9G). For this species, the microopits are arranged in a regular pattern. The diameter and depth of these are in the range of 300 nm and 50 nm, respectively (Fig. 9H).

Discussion and Conclusions

As outlined in the introduction, we speculated that spectacles might have self-cleaning properties, since snakes do not have eyelids or extremities to wipe their eyes. However, only polygonal-shaped structures surrounded by tiny borders that are some 10 nm high or deep are observed, in addition to micropits with diameters of some 100 nm and depths of some 10 nm. Therefore, the spectacles are extremely flat and feature only slightly hydrophobic contact angles around 100°. The adhesion forces measured with a sharp cantilever tip on the spectacles are higher than the values found on ventral and dorsal scales and confirm the observed contact angles. Due to these comparable low contact angles and high adhesion force values, we conclude that the examined snakes do not self-clean their eyes with the classical lotus effect. Consequently, they must clean their spectacles in other (unknown) ways or live on with possible contaminations. Over a longer period, snakes renew their dirty or worn spectacles along with ventral and dorsal scales by the periodical moulting process. Such a renewal process seems to be a sufficient cleaning strategy for snakes (the studied ones at least).

Another potential function of spectacles besides mechanical protection might be advanced optical transmittance. However, in agreement with previous studies, we observed no exceptional optical properties. The observed transmittance between 70% and 90% in the visible range appears to be sufficient for snakes, which's sensory system also relies on smelling, and potentially on infrared sensing. However, all examined spectacle scales block harmful UV rays in the UV-B and -C regime, as the transmittance reduces for wavelengths below 400 nm, finally diminishing close to zero for wavelengths below 300 nm. Nonetheless, a tiny-to-small transmission peak at 254 nm is observed in several spectra, reaching the highest values for the spectacles of *T. honsonensis* and *P. schultzei*. Our analysis revealed that this peak is not a true optical transmission; it is caused by the fluorescence of keratin around 254 nm.

Author Contributions

H. H. designed the study and wrote the final manuscript. W.W. and S.R. conducted the SEM, AFM, and optical spectroscopy experiments. F.B., R.T., and W.W. measured the wetting properties. G.G. collected the snake scales and took the photos shown in Figure 2. D.B. analysed the fluorescence effect. W.W. and S.R. wrote a first draft of the manuscript. All authors discussed the results and agreed on the final manuscript.

Acknowledgments

The authors thank Alban Muslija for support with the SEM analysis and Luisa Borgmann for her kind help with the optical spectroscopy measurements. The authors also acknowledge kind help in the lab by Cornelia Pichler and Patrick Weiser. The snake scale samples were kindly contributed by Christoph Rothenbühler, René Woning, Philippe Wolf, and Franz Gries. Nina Giraud kindly allowed us to photograph her *Python regius* snake "Cleopatra". W.W. gratefully acknowledges a scholarship from the China Scholarship Council (CSC). H.H. and D.B. gratefully acknowledge funding from the Helmholtz Association – Research Field Energy – Materials and Technologies for the Energy Transition program (Topic 1 Photovoltaics and Wind Energy, 38.01.05). This work was partly carried out with the support of the Karlsruhe Nano Micro Facility (KNMFi, www.knmf.kit.edu), an Open Access Research Infrastructure within the Karlsruhe High Technology Hub at the Karlsruhe Institute of Technology (KIT – The University in the Helmholtz Association, www.kit.edu). Finally, the authors acknowledge financial support through the "*Ideenwettbewerb Biotechnologie—Von der Natur lernen*" of the "*Ministerium für Wissenschaft, Forschung und Kunst Baden- Württemberg*"

References

Alvarez, J. A., Lewis-Deweese, P. and Wilcox, J. T. (2022). Ocular Biofluorescence Due to Ultra-violet Excitation in California Redlegged and Foothill Yellow-legged Frogs, in central California, USA. *Sonoran Herpetologist* **35**, 154–155.

Autumn, K. and Hansen, W. (2006). Ultrahydrophobicity indicates a non-adhesive default state in gecko setae. *J Comp Physiol A Neuroethol Sens Neural Behav Physiol* **192**, 1205–12.

Barthlott, W., Mail, M. and Neinhuis, C. (2016). Superhydrophobic hierarchically structured surfaces in biology: evolution, structural principles and biomimetic applications. *Philosophical Transactions of the Royal Society A* **374**, 20160191.

Botelho, L. M., Martins, S. E., Melocco, G., Toledo, L. F., Sazima, I. and Muscat, E. (2024). Fluorescence in amphibians and reptiles: new cases and insights. *Acta Herpetol.* **19**, 75–80.

Buck, F. (2020). Experimentelle Untersuchung der Benetzungseigenschaften von Schlangenschuppen.

Butt, H.-J. and Kappl, M. (2010). *Surface and Interfacial Forces*. Wiley-VCH.

Campbell, A. L., Bunning, T. J., Stone, M. O., Church, D. and Grace, M. S. (1999). Surface Ultrastructure of Pit Organ, Spectacle, and Non Pit Organ Epidermis of

Infrared Imaging Boid Snakes: A Scanning Probe and Scanning Electron Microscopy Study. *J Struct Biol* **126**, 105–120.

Cazalot, G., Rival, F., Linsart, A., Isard, P. F., Tissier, M., Peiffer, R. L. and Dulaurent, T. (2015). Scanning laser ophthalmoscopy and optical coherence tomography imaging of spectacular ecdysis in the corn snake (Pantherophis guttatus) and the California king snake (Lampropeltis getulus californiae). *Vet Ophthalmol* **18 Suppl 1**, 8–14.

Collin, H. B., Ha, M. H., Wagner, A., Folwell, M., Dunstan, N., Crowe-Riddell, J. and Collin, S. P. (2025). Surface Topography and Ultrastructure of the Spectacular Cells in the Eyes of Land and Sea Snakes (Squamata, Reptilia): Functional Adaptations of Micro-Ornamentation. *Journal of Morphology* **286**, e70084.

Da Silva, M. A., Bertelsen, M. F., Wang, T., Prause, J. U., Svahn, T. and Heegaard, S. (2016). Comparative morphology of the snake spectacle using light and transmission electron microscopy. *Vet Ophthalmol* **19**, 285–90.

Da Silva, M.-A. O., Heegaard, S., Wang, T., Gade, J. T., Damsgaard, C. and Bertelsen, M. F. (2017). Morphology of the snake spectacle reflects its evolutionary adaptation and development. *BMC Evolutionary Research* **13**, 258.

Guerra-Fuentes, R. A., Roscito, J. G., Nunes, P. M., Oliveira-Bastos, P. R., Antoniazzi, M. M., Carlos, J. and Rodrigues, M. T. (2014). Through the looking glass: the spectacle in gymnophthalmid lizards. *Anat Rec (Hoboken)* **297**, 496–504.

Hart, N. S., Coimbra, J. P., Collin, S. P. and Westhoff, G. (2012). Photoreceptor types, visual pigments, and topographic specializations in the retinas of hydrophiid sea snakes. *J Comp Neurol* **520**, 1246–61.

Lamb, J. Y. and Davis, M. P. (2020). Salamanders and other amphibians are aglow with biofluorescence. *Sci Rep* **10**, 2821.

Lauridsen, H., Da Silva, M. A., Hansen, K., Jensen, H. M., Warming, M., Wang, T. and Pedersen, M. (2014). Ultrasound imaging of the anterior section of the eye of five different snake species. *BMC Vet Res* **10**, 313.

Lillywhite, H. B. (2014). *How Snakes Work - Structure, Function and Behavior of the World's Snakes*. Oxford: Oxford University Press.

Paul, L. and Mendyk, R. W. (2021). Glow and Behold: Biofluorescence and new insights on the tails of pitvipers. *Herpetological Reviews* **52**,.

Prötzel, D., Heß, M., Scherz, M. D., Schwager, M., Padje, A. V. and Glaw, F. (2018). Widespread bone-based fluorescence in chameleons. *Sci Rep* **8**, 698.

Prötzel, D., Heß, M., Schwager, M., Glaw, F. and Scherz, M. D. (2021). Neon-green fluorescence in the desert gecko Pachydactylus rangei caused by iridophores. *Sci Rep* **11**, 297.

Reza, K. S. (2025). Control of Multifunctionalities of Nano and Microstructures.

Reza, K. M. S., Borgmann, L. M., Busko, D., Chen, J., Gunstheimer, H., Thelen, R., Gomard, G., Lemmer, U. and Hölscher, H. (2025). Nanopores in the ventral scales of *Bitis rubida* and *Bitis armata* cause white venters. *Biol Lett* **21**, 20250141.

Simoes, B. F., Sampaio, F. L., Douglas, R. H., Kodandaramaiah, U., Casewell, N. R., Harrison, R. A., Hart, N. S., Partridge, J. C., Hunt, D. M. and Gower, D. J. (2016). Visual Pigments, Ocular Filters and the Evolution of Snake Vision. *Mol Biol Evol* **33**, 2483–95.

van Doorn, K. (2012). Investigations on the Repilian Spectacle.

van Doorn, K. and Sivak, J. G. (2015). Spectral transmittance of the spectacle scale of snakes and geckos. *Contributions to Zoology* **84**, 1–12.

van Doorn, K. L. H., Sivak, J. G. and Vijayan, M. M. (2014). β-Keratin composition of the specialized spectacle scale of snakes and geckos. *Canadian Journal of Zoology* **92**, 299–307.

Walls, G. L. (1934). The Significance of the Reptilian "Spectacle." *American Journal of Ophthalmology* **17**, 1045–1047.

Wu, W. (2020). Tribological characterization of reptile scales and their application as technical surfaces with tunable friction anisotropy.

Wu, W., Yu, S., Schreiber, P., Dollmann, A., Lutz, C., Gomard, G., Greiner, C. and Hölscher, H. (2020). Variation of the frictional anisotropy on ventral scales of snakes caused by nanoscale steps. *Bioinspir Biomim* **15**, 056014.

413 **Table 1:** Summary of the investigated eighteen snake species belonging to five different families. The table gives binomial and common names,
414 geographical origin, observed contact angles and optical transmission values from shed skin. Some dorsal scales were too small (diameter of single
415 scale < 1 mm) to conduct reliable contact angle measurements, and these missing values are shown as n/a.

416

Binomial name(s)	**Common Name**	**Origin**	**Family**	**Comment**	**Contact angle of single scale**			**Spectroscopic parameters of spectacle scale**	
					Dorsal	**Ventral**	**Spectacle**	$\lambda_{50\%}$	$T_{@750\ nm}$
Sisturus milarius barbouri	Dusky Pygmy Rattle Snake	North America	Viperidae	Terrestrial	143 ± 5°	111 ± 3°	103 ± 3°	306 nm	87.6%
Pantherophis guttatus	Eastern Corn Snake		Colubridae	Terrestrial	133 ± 2°	108 ± 1°	98 ± 6°	305 nm	87.4%
Zamenis situla	European Rat Snake	Europe	Colubridae	Terrestrial	n/a	108 ± 4°	97 ± 2°	322 nm	86.6%
Natrix helvetica	Barred Grass Snake		Colubridae	Semi-aquatic	n/a	72 ± 16°	91 ± 1°	328 nm	88.8%
Natrix tessellata	Dice Snake		Colubridae	Semi-aquatic	n/a	108 ± 5°	87 ± 4°	322 nm	75.6%
Malpolon monspessulanus	Montpellier Snake		Psammophiidae	Terrestrial	130 ± 7°	118 ± 5°	101 ± 3°	330 nm	88.5%
Vipera ursinii rakosiensis	Hungarian Meadow Viper		Viperidae	Terrestrial	123 ± 2°	106 ± 4°	109 ± 1°	311 nm	81.8%

Vipera aspis	Aspic Viper		Viperidae	Terrestrial	141 ± 4°	111 ± 1°	103 ± 1°	312 nm	90.1%
Vipera seoanei	Seoane's viper		Viperidae	Terrestrial	n/a	107 ± 3°	110 ± 2°	310 nm	78.7%
Vipera lotievi	Lotiev's Viper	Eastern Europe	Viperidae	Terrestrial	n/a	112 ± 1°	109 ± 3°	317 nm	80.7%
Vipera renardi	Steppe Viper	Western and Central Asia	Viperidae	Terrestrial	n/a	108 ± 1°	101 ± 3°	307 nm	82.5%
Parias schultzei (Trimeresurus schultzei)	Schultze's Pitviper	Asia	Viperidae	Arboreal	134 ± 2°	107 ± 3°	106 ± 3°	301 nm	86.3%
Trimeresurus honsonensis	Hon Son pit viper		Viperidae	Arboreal	125 ± 3°	103 ± 2°	100 ± 2°	303 nm	77.3%
Tropidolaemus subannulatus	North Philippine Temple Pitviper		Viperidae	Arboreal	wetting	60 ± 7°	107 ± 2°	307 nm	82.7%
Naja atra	Chinese Cobra		Elapidae	Terrestrial	122 ± 4°	111 ± 1°	102 ± 2°	385 nm	88.4%
Morelia spilota	Carpet Python	Oceania	Pythonidae	Mostly arboreal	134 ± 6°	108 ± 2°	92 ± 2°	306 nm	83.7%
Bitis arietans	Puff Adder	Africa and south-west of Arabian Peninsula	Viperidae	Terrestrial	145 ± 3°	59 ± 3°	104 ± 2°	324 nm	89.5%
Spalerosophis diadema	Diadem Snake	Africa	Colubridae	Terrestrial	126 ± 5°	109 ± 2°	96 ± 6°	330 nm	89.9%

417

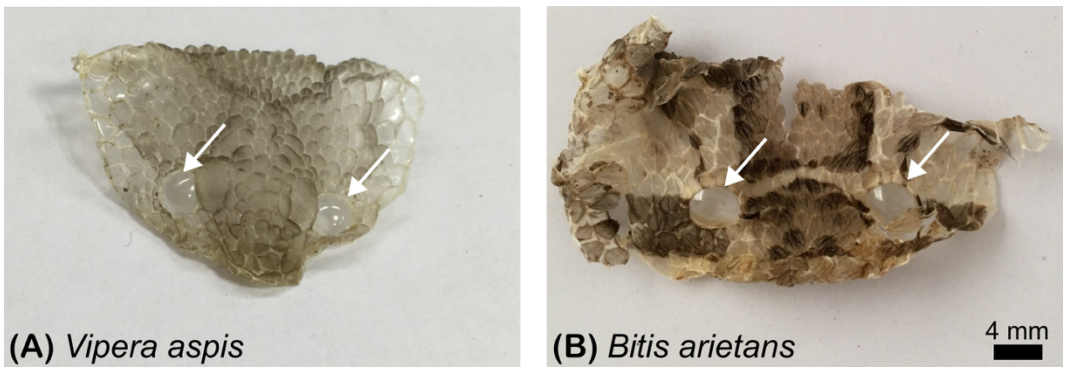


Figure 1: Photographs of the moulted head scales of (A) *Vipera aspis* and (B) *Bitis arietans*. The spectacles (marked by white arrows) protecting the eyeballs are much more transparent than the other head scales. The spectacles of *B. arietans* (about 5 mm in diameter) are slightly larger than the ones of *V. aspis* (about 4 mm in diameter).

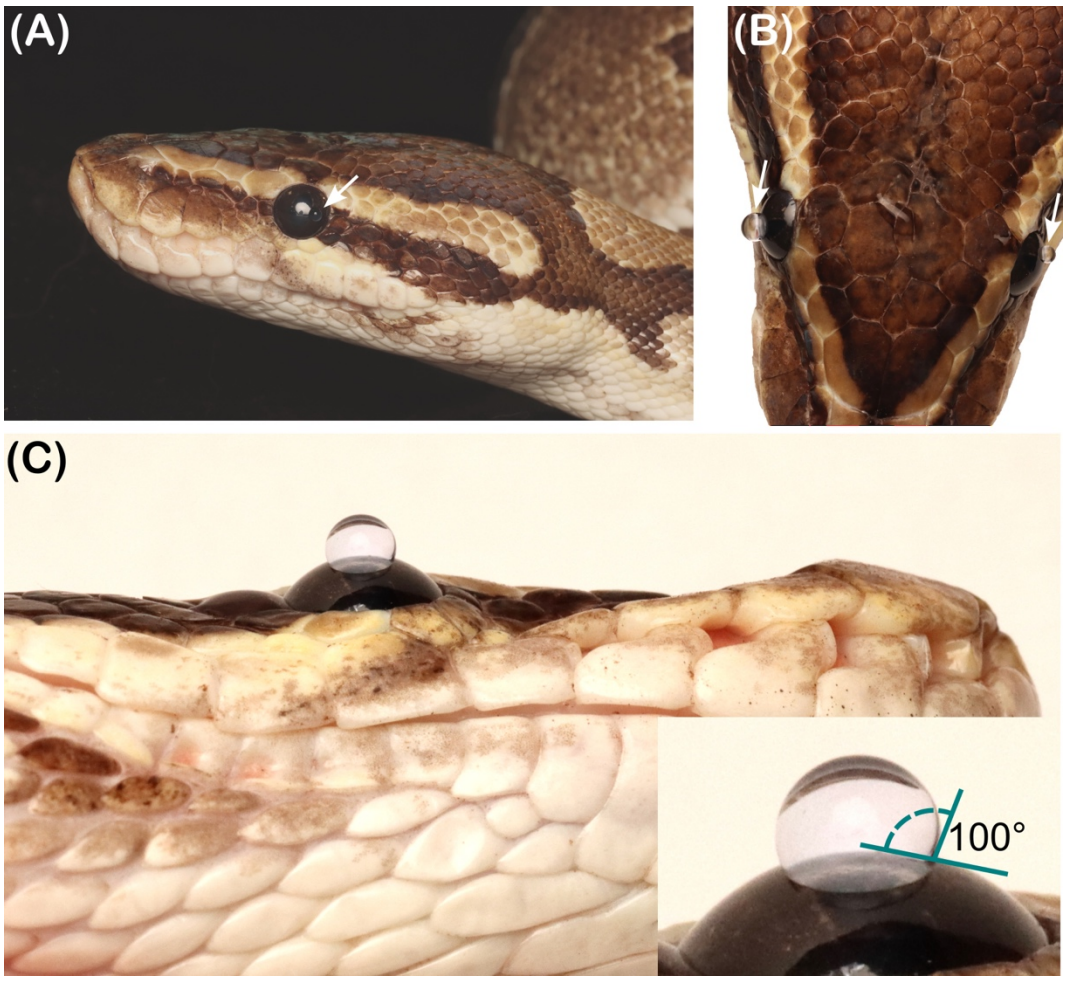


Figure 2: Photographs (background removed in (B) and (C)) of water droplets sticking to the spectacle scales of a living *Python regius* about three weeks after her last shedding. (A) Portrait view of the snake's head. The white arrow marks a small droplet of water sticking to the left spectacle of the snake. (B) Top view of the same snake, showing two water droplets sticking to

both spectacles, respectively. (C) A side view of the water droplet sticking to the right spectacle shows that the contact angle is larger than 90°, roughly about 100° (see inset).

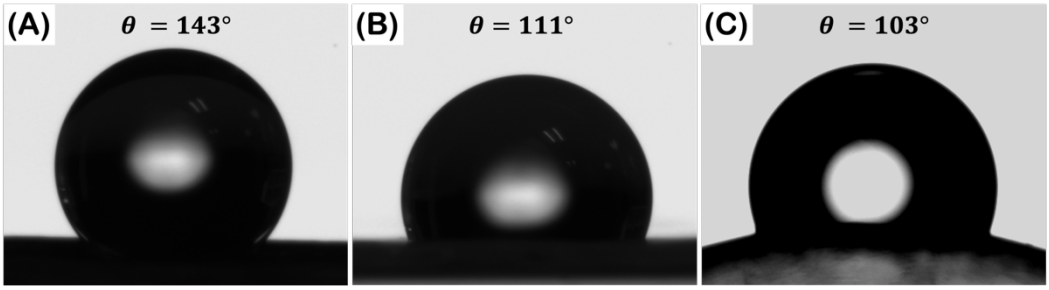


Figure 3: Water contact angle measurements conducted on (A) dorsal, (B) ventral, and (C) spectacle scales of *S. m. barbouri* with a 1 µL droplet of water**.** Interestingly, the contact angle on the spectacle is lowest.

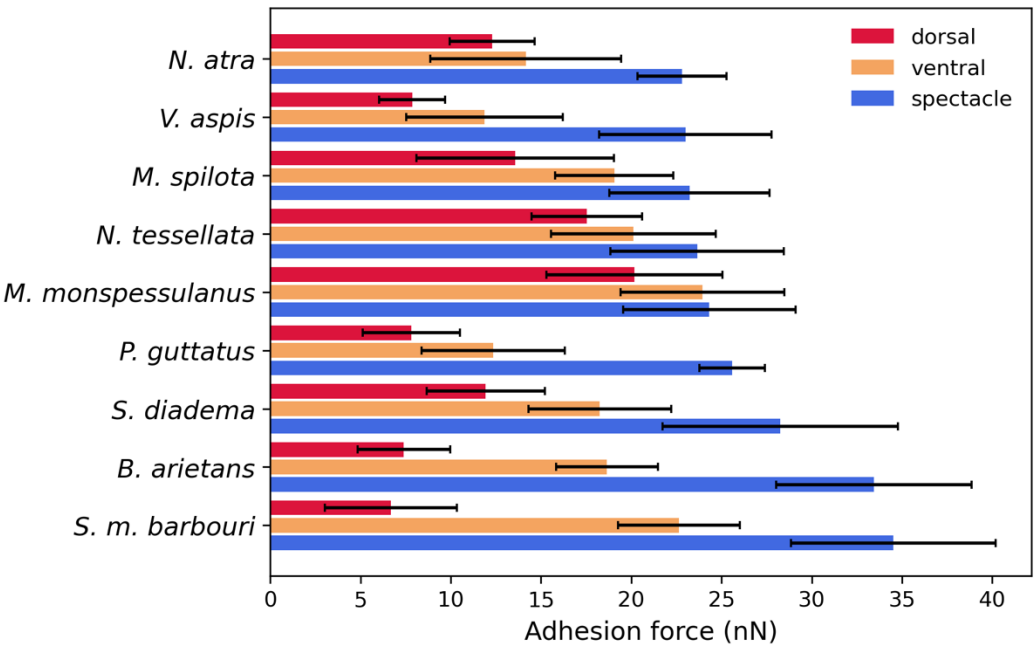
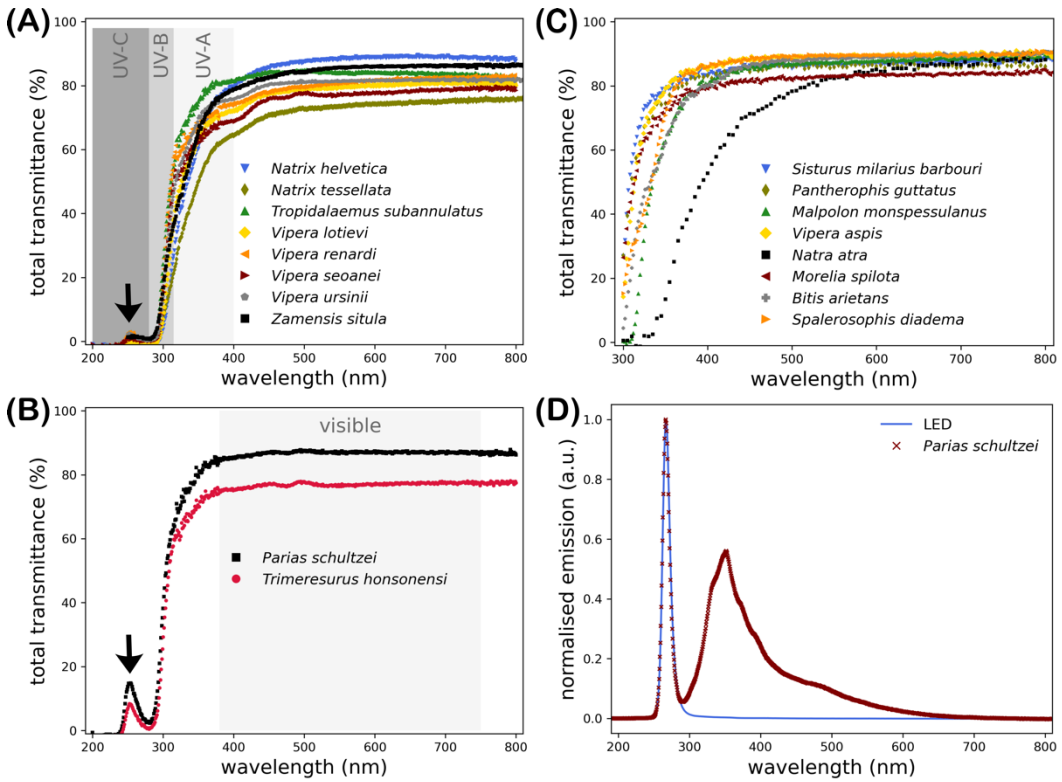


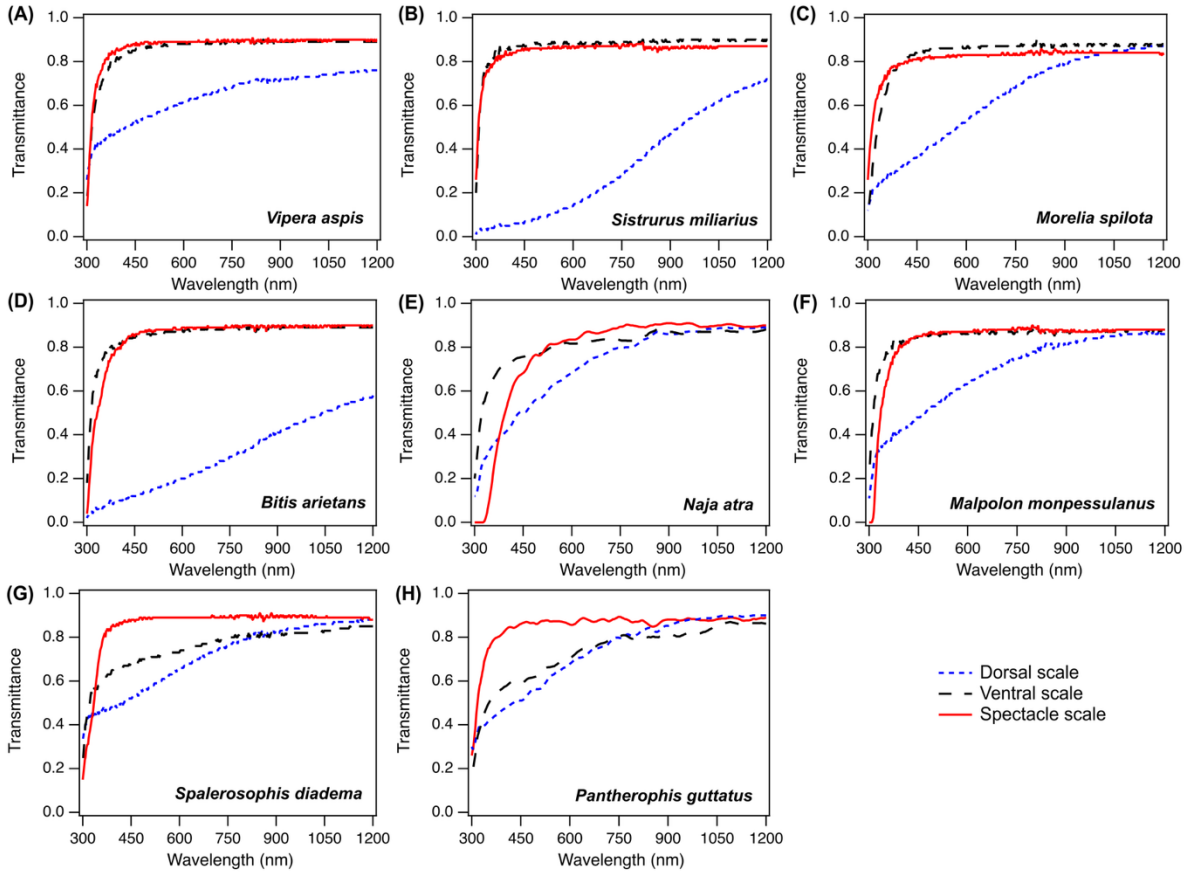
Figure 4: Comparison of the adhesion forces recorded on the dorsal, ventral, and spectacle scales of a sub-collection of the examined species. The adhesion forces were measured 10 times by atomic force microscopy with a sharp silicon tip at 10 arbitrarily chosen positions. The overall average adhesion force of all 100 measurements was calculated, and the error bars correspond to the standard deviation. In general, the adhesion force is highest on the spectacle scales, lowest on dorsal scales, and intermediate on ventral ones.



443

444 **Figure 5:** (A) Optical transmittance of the spectacle of 8 snake species for wavelengths between
445 200 and 800 nm. The transmittance is between 70% and 90% in the visible regime between 380
446 nm and 750 nm, and is significant in the UV-A region but decays strongly in the UV-B before
447 it reduces to nearly zero for wavelengths below 300 nm in the UV-C regime. (B) The spectra
448 of *P. schultzei* and *T. honsonensis* are plotted in an additional graph to emphasize the peak
449 around 254 nm (see black arrow). The visible regime of humans is indicated for comparison
450 only. (C) The spectral transmittance for the rest of the spectacles was measured in the range
451 from 300 nm to 800 nm. The curves show the same overall shape as in (A) and (B). (D) The
452 spectrum of the UV LED utilized for the excitation of a dorsal scale of *P. schultzei* is plotted as
453 a solid line. The resulting fluorescence spectrum caused by this excitation is shown as symbols.

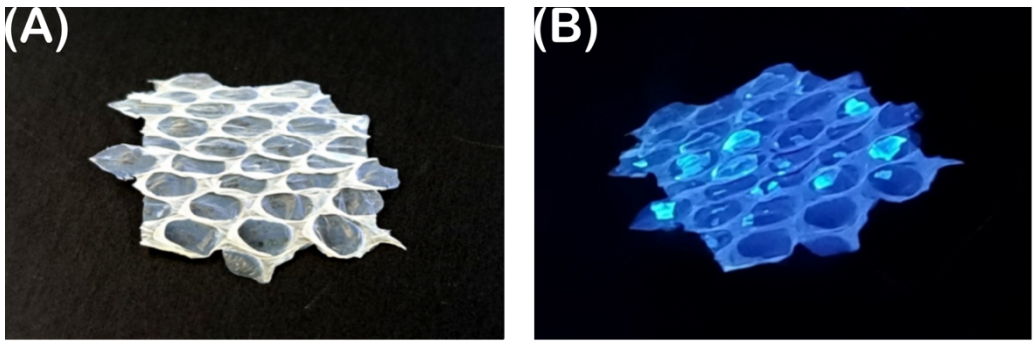
454



455

456 **Figure 6:** Comparison of the total spectral transmittance of dorsal, ventral, and spectacle scales
457 for 8 different species. (A) *Vipera aspis,* (B) *Sistrurus miliarius barbouri,* (C) *Morelia silota,*
458 (D) *Bitis arietans,* (E) *Naja atras,* (F) *Malpolon monpessulanus,* (G) *Spalerosophis diadema,*
459 (H) *Pantherophis guttatus*. As the dorsal scales typically contain pigments like melanin, their
460 transmission values are typically lower as for the ventral and spectacles scales. However, in the
461 cases (A) to (F), the total transmittance of the pigment-free ventral scales is comparable to that
462 of the spectacles.

463

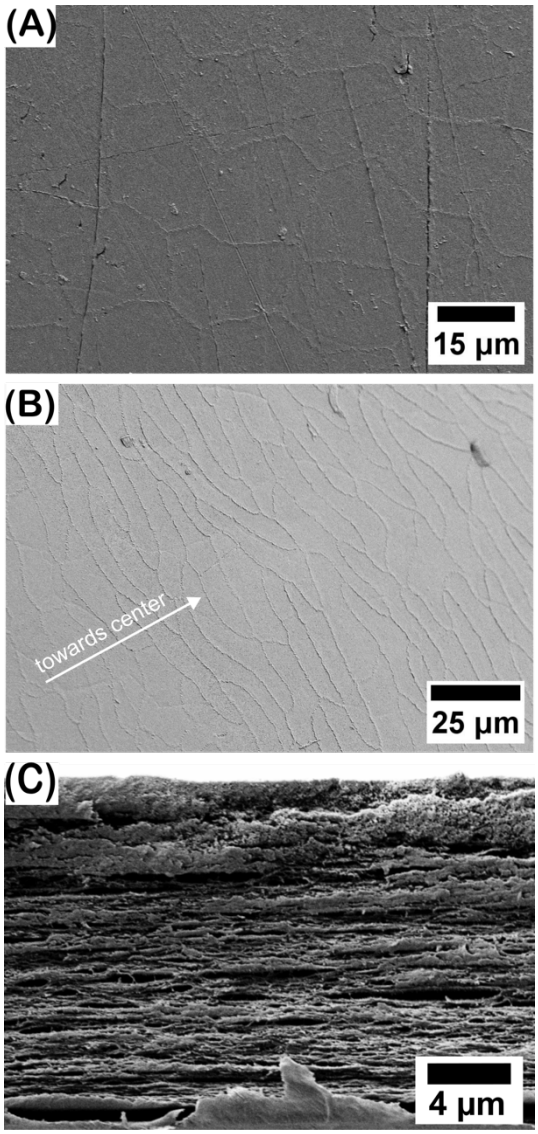


464

465 **Figure 7:** Comparison of two photos of dorsal scales of *Parias schultzei* taken under (A)
466 ambient and (B) UV (268 nm) light on top of a black substrate. The photos were taken with a

467 smartphone camera. For the UV excitation photo, the following manual settings were applied:
468 ISO 3200, F1.8, 1/30s, WB 4300K.

469



470

471 **Figure 8:** SEM images of the spectacle of *P. guttatus* recorded (A) in the centre and (B) near
472 the edge reveal pentagonal or hexagonal patterns formed by elevated borders on the exterior
473 surface. The white arrow in (B) indicates the direction towards the centre of the spectacle. (C)
474 The cross-section of the spectacle shows thin dense layers but no dedicated structure.

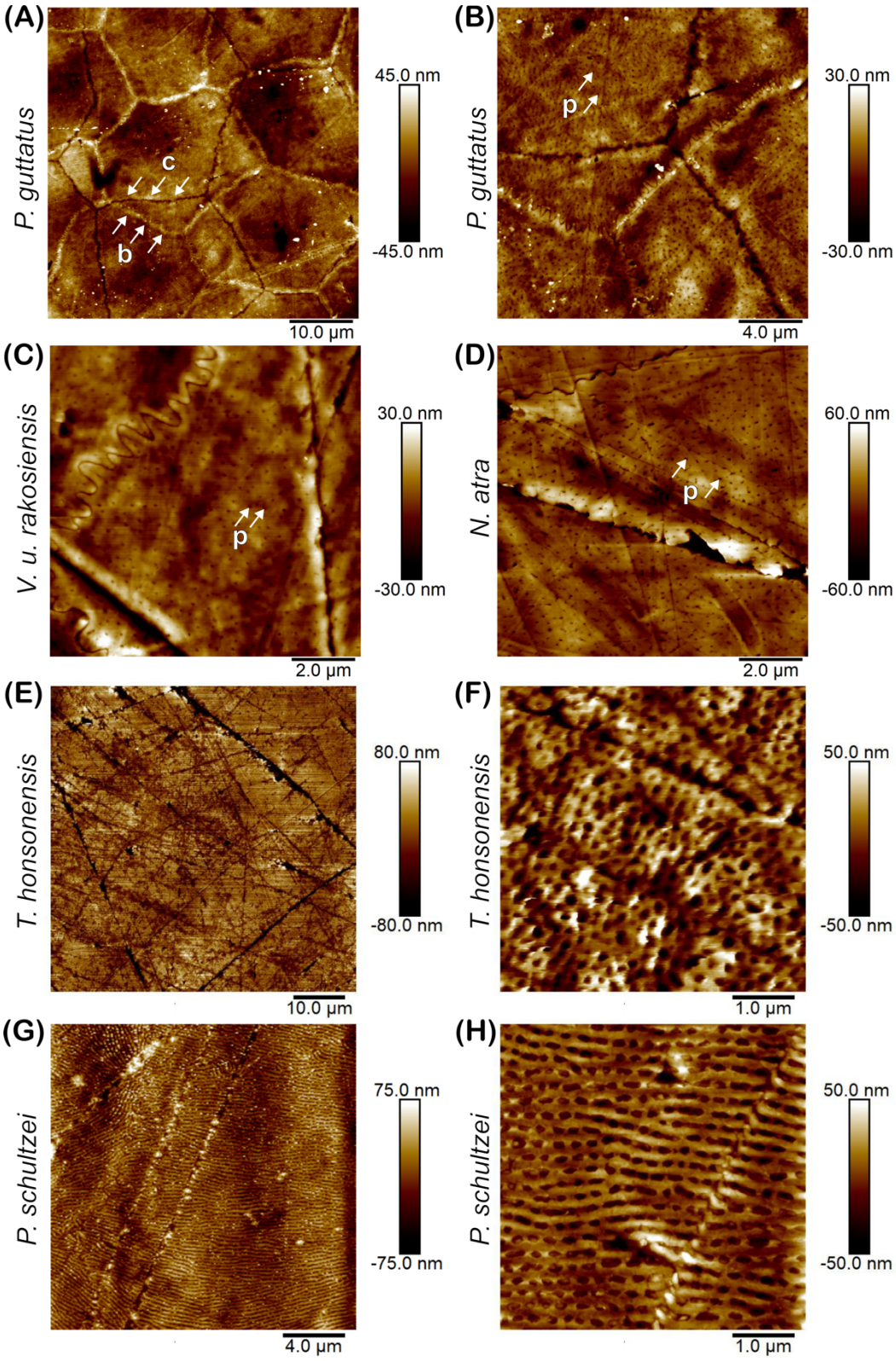


Figure 9: Examples of nanoscale structures observed by AFM on spectacles of various snake species. A) An AFM image recorded in the centre of a spectacle scale of *P. guttatus* reveals narrow channels as depressions (marked as c) and additional border type in addition to the elevated borders (marked as b) which were already visible in the SEM images shown in Fig. 8A) and B). (B) An enlargement of (A) reveals further details. All flat areas of the scale of *P.*

guttatus are covered with nanoscale pits (marked as p). The AFM images of the spectacles of (C) *V. u. rakoseinsis* and (D) *N. atra* reveal flat surfaces with numerous micropits. White arrows exemplarily indicate two nanoscale pits (marked as p) in both images. (E) The topography measured by AFM reveals micropits on the spectacles of *T. honsonensis*. In difference to the spectacles of *P. guttatus,* narrow channels or stitching boundaries are not prominent. However, several cracks and scratches can be spotted on the surface. (F) A higher resolution image reveals a high density of micropits on the surface. (G) An overview AFM image of the scale of *P. schultzei.* (H) An image, taken with higher resolution, reveals the diameter and depths of micropits, which are roughly 300 nm and 30 nm, respectively.